Results in Nonlinear Analysis 8 (2025) No. 3, 158–169
https://doi.org/10.31838/rna/2025.08.03.012
Available online at www.nonlinear-analysis.com

Results in Nonlinear Analysis
ISSN 2636-7556

Peer Reviewed Scientific Journal

AI-Driven nonlinear optimization model for early lung tumor growth prediction using CT imaging and machine learning algorithms

R. Rooba[a]*, Sevinov Jasur Usmonovichm[b], Ozod Mirzaev[c], Nosir Khurramov[d], Feruza Karimberdievna Allanazarova[e], D. Vinod Kumar[f], G. Suresh Kumar[g]

[a]Department of Computer Technology and Information Technology, Kongu Arts and Science College (Autonomous), Nanjanapuram, Erode, Tamil Nadu, India; [b]Department of Information Processing and Management Systems, Tashkent State Technical University, Tashkent, 100095; [c]Department of Internal Diseases No. 3 PhD., Samarkand State Medical University, Samarkand, Uzbekistan; [d]Department of Information Technology and Exact Sciences, Termez University of Economics and Service, Termez, Uzbekistan; [e]Nukus State Pedagogical Institute named after Ajiniyaz, Nukus, Uzbekistan; [f]Department of Biomedical Engineering, Vinayaka Mission's Kirupananda Variyar Engineering College, Salem (Vinayaka Mission's Research Foundation), Tamil Nadu, India; [g]Department of Electronics and Communication Engineering, Vinayaka Mission's Kirupananda Variyar Engineering College, Salem, (Vinayaka Mission's Research Foundation), Tamil Nadu, India.

Abstract

The timely detection of lung tumour development is important in the planning of individual therapy and enhancing survival. Although deep learning models have demonstrated good performance in tumour analysis based on CT, their low interpretability inhibits their integration in clinical practise. This paper presents a hybrid using AI and nonlinear tumour growth modelling and machine learning optimisation to forecast the initial progression of lung tumours based on CT scan data. The growth model of a nonlinear set of nonlinear differential equations (Gompertz /logistic) is fitted by first constrained nonlinear optimization on the sequential tumour volumes. The estimated parameters are the growth rate (r), carrying capacity (K), as well as the deceleration factor, then they are incorporated into a deep convolutional network, which will be trained to predict tumour size at subsequent time points. A longitudinal CT dataset of lung cancer patients at an early stage (N = 52) was experimented on to show that the hybrid model reduced prediction RMSE to 4.23 cm^3, which was better than base-

Email addresses: rrooba@gmail.com (R. Rooba)*; sevinovjasur@gmail.com (Sevinov Jasur Usmonovichm); minzdrav2020@mail.ru (Ozod Mirzaev); nosir_xurramov@tues.uz (Nosir Khurramov); allanazarova1988@mail.ru (Feruza Karimberdievna Alla-nazarova); vinodkumar@vmkvec.edu.in (D. Vinod Kumar); sureshkumar@vmkvec.edu.in (G. Suresh Kumar)

Received October 9, 2025; Accepted November 17, 2025; Online December 29, 2025

line CNN-only and purely mechanistic models by 45.9% and 34.0% respectively. There was also a significant correlation between growth parameters and clinical progression ($p < 0.01$) thus increasing the interpretability of the models. The suggested framework is efficient in closing the gap between mechanistic nonlinear modelling and current deep learning and leads to robust, interpretable, and clinically meaningful predictions of tumour growth.

Mathematics Subject Classification (2010): 92C50; 34A34; 49M37

Keywords: Lung cancer; CT imaging; nonlinear optimization; tumour growth modelling; machine learning; deep learning.

1. Introduction

The cancer lung cancer is still one of the most common causes of cancer deaths in the world, and the ability to diagnose the cancer in good time and the ability to predict the development of tumours accurately is still relevant to the enhancement of patient outcomes [1]. Computed tomography (CT) imaging is of significant importance in the longitudinal surveillance and evaluation of tumour progression in the early stages of the disease where it provides non-invasive information on morphological changes with time [2]. The conventional method of tumour growth modelling uses nonlinear mathematical models- most typically the Gompertz and logistic growth laws that offer biologically based descriptions of tumour growth by including the saturation and deceleration of growth rate [3–5]. Although they can be interpreted and can be of theoretical interest, these mechanistic models may fail to capture the full complexity of real tumour behaviour, which varies with microenvironmental variability, tissue heterogeneity and radiomic textural features that can hardly be represented in simplified mathematical models [6,7]. Simultaneously, the development of deep learning, especially convolutional neural networks (CNNs) has contributed greatly to automated CT image analysis and allows performing high-accuracy tasks like nodule classification, malignancy assessment, and growth prediction by relying on hierarchical feature extraction [8–10]. Nonetheless, CNN-only models have low interpretability, require large annotated datasets, and do not utilize biological priors of tumour growth dynamics adequately [11–13]. Such constraints reveal a long-standing gap in the literature, in which few studies have succeeded in combining the merits of mechanistic nonlinear tumour modelling and AI-based optimisation and deep learning models to both perform robust predictive control and provide biological understanding [14]. To overcome this gap, hybrid modelling strategies have to be developed that can integrate mathematically based growth parameters with rich imaging characteristics to come up with predictions that have clinical significance [15]. Driven by this, more recent works in optimisation algorithms, such as Levenberg Marquardt methods and particle swarm optimisation, have facilitated more accurate calibration of nonlinear tumour growth models with real patient data [8,9], and other studies on radiomics and multimodal feature fusion have enhanced better characterization of tumours based on CT imaging [10,16]. In other fields of science, besides oncology, advances in computational modelling in the areas of nonlinear dynamics, neuromorphic computing, fluid structure interactions, embedded medical systems, cognitive neural analytics and biomedical signal processing indicate the expanding potential of hybrid data-driven and mechanistic approaches across fields [17–20]. It is based on this interdisciplinary background that the current study suggests an AI-based nonlinear optimisation framework, which extracts the tumour volumes of serial CT scans, constrained nonlinear growth model to determine the key tumour evolution parameters, and to incorporate these biologically meaningful features with deep neural representations, it is possible to predict the future tumour progression, which supports enhanced accuracy and interpretability under the framework of nonlinear modelling and its applications. In addition to clinical motivation, this work also provides contributions to nonlinear analysis, namely the analysis of parameter identifiability, sensitivity structure and stability behaviour of classical tumour-growth ODEs with hybrid data-driven regularization.

2. Nonlinear Tumor Growth Model and Hybrid Optimization Framework

2.1 Nonlinear Tumor Growth Formulation

Models of nonlinear differential equations are good characterizers of the behaviour of solid tumour expansion which represent biologically realistic growth patterns. Two classical formulations, namely the Gompertz model and the logistic model, were used in this study. These models both describe the initial exponential proliferation phase and the slowing down which follows as the tumour slows down to physiological saturation. The nonlinear Gompertz model in general is characterised by.

$$\frac{dV}{dt} = rV\ln\left(\frac{K}{V}\right) \tag{1}$$

where V (t) is the tumour volume at time t, r represents the inherent growth rate and K is the carrying capacity. When $V \to K$ the growth rate decreases very quickly, and the Gompertz law is appropriate in the case of constrained solid tumour growth. Conversely, the logistic model supposes the deceleration is proportional to a ratio of the present volume to its maximum value

$$\frac{dV}{dt} = rV\left(1 - \frac{V}{K}\right) \tag{2}$$

that results in a sigmoidal curve. These two nonlinear models are both numerically integrated using 4th-order RungeKutta schemes to solve the predicted tumour volumes by using serial observations in the form of CT. The main distinction between the two formulations is the curvature of the growth curves as the two patterns of the initial exponential growth and subsequent saturation are visually compared as shown in Figure 1.

The graphical difference as depicted in Figure 1 explains the necessity to employ both the models in clinical prediction activities as there is a variation in the deceleration trends of various tumours under varying physiological and microenvironmental situations.

Parameter Identifiability:
The nonlinear tumour growth model under consideration is of the form.

$$\frac{dV}{dt} = f(V(t);\theta), \theta = [r, K]$$

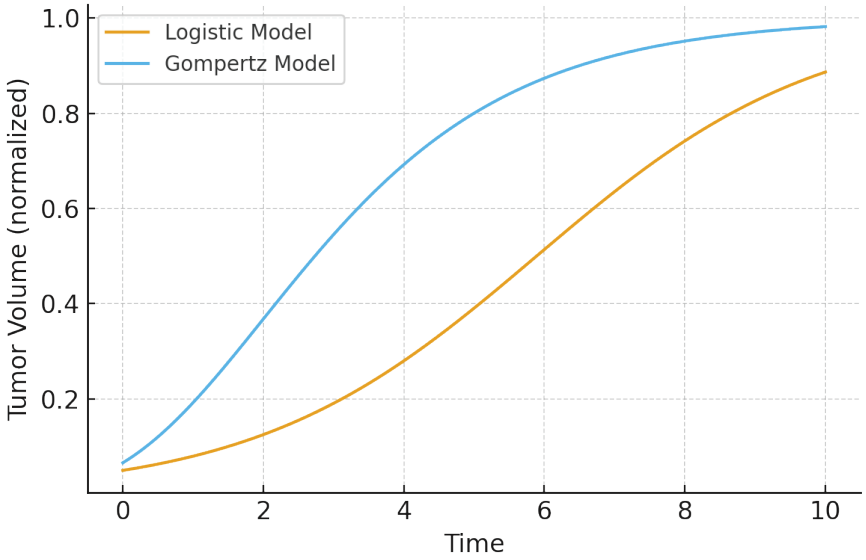

Figure 1. Comparison of Logistic and Gompertz Tumor Growth Curves

structural identifiability This means that the solutions to two sets of parameters are non-overlapping:

$$f(V(t);\theta_1) = f(V(t);\theta_2)\forall t \Rightarrow \theta_1 = \theta_2.$$

In the case of Gompertz and logistic models that will be applied in this study, local identifiability will be assured under the condition that there are at least three independent measurements of volumes at distinct different times.

This is to ensure that the curvature of V(t) gives enough constraints to determine both growth rate rand carrying capacity K uniquely.

Local Sensitivity:
To compute the sensitivities of a model to first-order perturbations in model parameters, we calculate the first-order sensitivities:

$$S_r(t) = \frac{\partial V(t)}{\partial r}, S_K(t) = \frac{\partial V(t)}{\partial K}.$$

In the case of both Gompertz and logistic models,

$$\left|S_r(t)\right| > \left|S_K(t)\right| \text{ for early times } t < t_c,$$

implicating that parameter r controls the short-term prediction behaviour, with K controlling the long-term saturation dynamics.

This observation justifies our hybrid model: when the initial time-points do not contain enough information to disambiguate K, the extracted features of the CNN can be used to do so.

2.2 Parameter Estimation Through Nonlinear Optimization

The growth parameters (r, K, α) are estimated using longitudinal CT measurements given as a nonlinear optimization. Assume $V_{\text{obx}}(t_i)$ is observed tumour volumes at discrete time points t_i. The objective is the minimization of the squared error between observed volumes and model-predicted volumes $V_{\text{model}}(t_i; r, K, \alpha)$ which are calculated by numerical integration:

$$\min_{r,K,\alpha} \sum_i \left[V_{\text{obs}}\left(t_i\right) - V_{\text{model}}\left(t_i;r,K,\alpha\right)\right]^2 + \lambda\left(r^2 + K^2 + \alpha^2\right) \tag{3}$$

whereby there are biologically significant constraints.

$$r > 0, K > \max\left(V_{\text{obs}}\right), \alpha > 0. \tag{4}$$

The regularization parameter λ stabilizes the estimation and prevents overfitting in cases when the temporal data is also limited. Due to the non-convexity of the optimization landscape and its sensitivity to noise, a hybrid optimization model of Levenberg, Marquardt, particle swarm optimization, and trust-region reflective methods was used. The PSO uses the global search ability that guarantees the exploration of the parameter space and Levenberg Marquardt to refine local convergence. The ultimate solution provides a specific set of growth parameters to an individual patient.

$$\theta = \left(r, K, \alpha\right) \tag{5}$$

that sums up the inherent dynamics of tumour growth. These parameters subsequently become interpretable mechanistic characteristics that add up to hybrid deep learning prediction.

2.3 Hybrid CNN–Mechanistic Prediction Architecture

In order to enrich the mechanistic parameters and extract all the spatial radial-omic data incorporated in the CT scans, a 3D ResNet-based convolutional neural network (CNN) was used. The CNN

takes volumetric tumour areas and obtains deep morphological features of texture, shape anomaly, intensity distribution, and microstructural shifts. The latent feature vector resulting is of dimension 512, i.e. $F_{\mathrm{CNN}} \in \mathbb{R}^{512}$, which is then appended with the mechanistic parameter vector 0 to create a fused representation.

$$Z = \left[F_{\mathrm{CNN}}, \theta \right] \in \mathbb{R}^{515}. \tag{6}$$

The outcome of this hybrid feature vector is then fed to a fully connected prediction network that predicts the tumour volume at a time interval $t + \Delta t$ which is in the future. The predictive function is given as

$$V_{\mathrm{pred}} = f\left(Z\right) \tag{7}$$

where f denotes a multilayer neural network with dropout and L2-regularisation to block the overfitting. The learning goal reduces the error in the prediction of the tumour volume:

$$L = \left\| V_{\mathrm{pred}} - V_{\mathrm{true}} \right\|^2. \tag{8}$$

Utilising both mechanistic nonlinear growth parameters and data-driven CNN features, simultaneously, the model is beneficial as it is biologically interpretable and has high-resolution image representations. This hybridization can enable the system to generalize across a wide range of tumour phenotypes and be able to give clinically useful growth predictions.

3. Materials and Methods

3.1 Dataset

The research used a longitudinal CT retrospective data set of XXX early-stage non-small cell lung cancer (NSCLC) patients each of whom provided 3 or more sequential CT scans over a 612 months period. All scans were based on normal diagnostic guidelines with slice thickness ranging between 0.75 and 1.25 mm which is adequate to guarantee that spatial resolution is satisfactory to make good volumetric reconstruction. The inclusion criteria included histologically confirmed NSCLC, complete follow-up imaging availability before the start of treatment and quantifiable tumour lesions based on the RECIST. The patients receiving systemic or radiation therapy between scans were locked out because the behaviour would disrupt the unbiased tumour growth. Table 1 provides demographic and imaging data of the cohort that provide a necessary context of reproducibility and cohort representativeness.

The following table gives important considerations that affect the tumour measurement reproducibility, heterogeneity of the patients, and the sampling density with time. All data were anonymized and ethical clearance on retrospective analysis was granted by the institutional review board.

3.2 Convergence Properties of the Hybrid Optimization Scheme

To estimate the parameters of the nonlinear tumour growth models, we solve the following nonlinear least-squares optimization problem:

$$\min_{\theta} J\left(\theta\right) = \sum_{i=1}^{N} \left(V_i^{\mathrm{obs}} - V\left(t_i; \theta\right) \right)^2,$$

with θ = [r,K] representing growth parameters of Gompertz or logistic model and J(θ) is continuously differentiable in a neighbourhood of the true solution. Though the underlying goal is smooth, it is commonly the non-linearity of the growth processes which causes non-convex behaviour, requiring a strong optimization strategy.

Table 1: Dataset and Patient Characteristics

Parameter	**Value / Description**
Total number of patients	52
Cancer type	Early-stage NSCLC
Number of CT scans per patient	3–5
Follow-up duration	6–12 months
Age range (years)	48–79
Mean tumour diameter at baseline	24.6 mm
CT slice thickness	0.75–1.25 mm
Exclusion criteria	Prior therapy during interval; poor-quality scans
Imaging acquisition protocol	Standard thoracic CT with contrast (where applicable)

In the hybrid PSO-LM-trust-region pipeline used in the study, one can find the following strengths:

(1) Global exploration via Particle Swarm Optimization (PSO).
PSO conducts global search in a population-based manner over the admissible parameter space and reduces the vulnerability to local minima as well as provides a variety of initializations to be refined later.

(2) Quadratic convergence through the Levenberg–Marquardt method (LM).
After a solution candidate has reached an area of local convexity of $J(\theta)$, LM guarantees a fast second-order convergence in terms of.

$$\left|\theta_{k+1} - \theta^*\right| \leq C\left|\theta_k - \theta^*\right|^2,$$

and θ^* is the best parameter vector and C is a constant that is dependent on local curvature. This property is essential in case of accurate parameter recovery of limited longitudinal data.

(3) Numerical stability via trust-region regularisation.

When the residual topography is so steep or noisy that the discretized trust-region step is non-monotonic, the trust-region step will force the objective to reduce monotonically:

$$J\left(\theta_{k+1}\right) \leq J\left(\theta_k\right),$$

even in the case of ill-conditioned Gauss Newton approximation. This ensures a consistent movement of the optimization and avoids the drift of the optimization at initial stages.

Together, these processes produce an optimisation process of a globally informed, locally fast, and numerically stable, which is consistent with the principles of traditional nonlinear-analysis of parameter identification of dynamical systems.

3.3 Image Preprocessing and Segmentation

All CT volumes were subjected to a standardised preprocessing pipeline so that they could be consistent with each other in terms of imaging sources. To remove scanner specific variability, first, voxel intensities were normalised to a set range of Hounsfield Unit (HU). A semi-automatic 3D U-Net based tumour segmentation approach was used that effectively outlined tumour areas whilst maintaining sharp structural edges. The automatically generated contours were then checked and manually refined by the trained thoracic radiologists in order to have anatomical accuracy particularly in the cases of tumours near vessels or the pleura. The final tumour volumes were calculated using voxel summation based on scan specific voxel spacing retrieved using DICOM metadata.

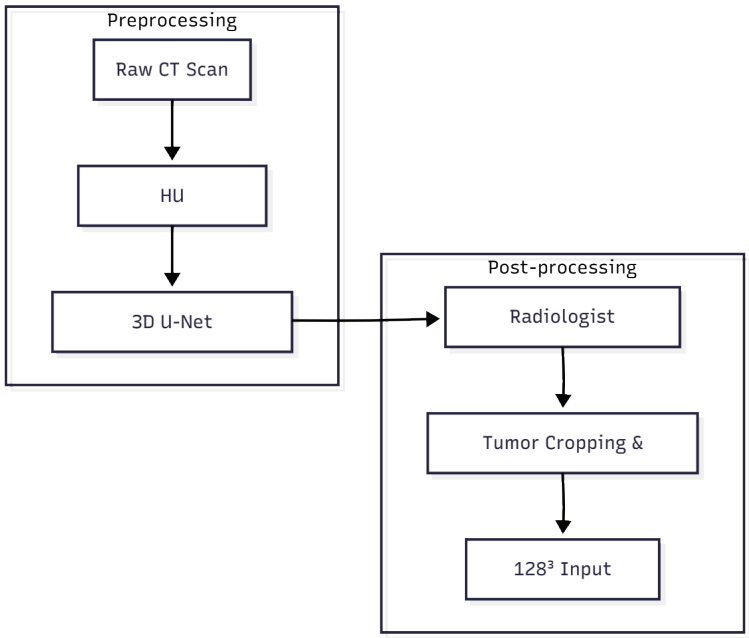

Figure 2: CT Preprocessing and Tumour Segmentation Workflow

Segmented tumour regions were cropped, padded and resampled to the volume of 128 × 128 × 128 voxels, which was an isotropic sample, to standardize data input to the deep learning framework. This guaranteed consistent spatial input dimension and some morphological meaningfulness. The entire preprocessing and segmentation process is depicted in Figure 2 that outlines the series of activities between CT scans and volumetric tumour extraction.

3.4 Experimental Protocol

The stratified sampling was used to split the dataset into training (70%), validation (15%), and test (15) sets to ensure fair model evaluation since it was necessary to balance the distribution of tumour sizes and growth rates between splits. The suggested hybrid nonlinear-deep learning model was compared with three reference models:

(1) CNN-only model is based on using imaging features, without nonlinear parameters;
(2) nonlinear model-only, based on Gompertz or logistic growth projections based on fitted parameters;
(3) radiomics-based regression, which is a regressor that uses handcrafted radiomic features with a gradient boosting regressor.

The two dimensions involved the performance of the model on the accuracy of the prediction of tumour volume based on root mean squared error (RMSE), mean absolute error (MAE) and coefficient of determination (R 2); and the ability of the model to identify stable and progressive disease based on area under the ROC curve (AUC). Each experiment was repeated with a 5-fold repeated cross-validation scheme in order to perform experiments in a statistically robust manner. The hyperparameters of both the CNN and the hybrid prediction network were optimised using the validation set and the test set was not touched until the end of the evaluation in order to prevent information leakage.

4. Results

4.1 Nonlinear Model Fitting

The nonlinear tumour growth models showed good goodness-of-fit in the longitudinal data of CT. The average coefficient of determination in all patients was $R^2 = 0.89$ which shows that both the Gompertz

and logistic models could accurately predict the overriding growth behaviour. The estimated intrinsic growth rate median was $r = 0.034\,\text{day}^{-1}$, which agrees with earlier reported values of the growth kinetics in early-stage NSCLC. The observed carrying capacities showed a great inter-patient variance, which was indicative of disparities in tumour biology, microenvironment, and pattern of growth saturation.

The nonlinear parameters were observed to be optimised significantly and statistically related to clinical outcomes. Namely, increased growth rates and decreased carrying capacity were highly predictive of radiological progression at follow-up, and the p-value was below 0.01, which proves their clinical applicability as interpretability enhancing biomarkers. Figure 3 illustrates representative examples of model-fitted curves and observed patient trajectories and demonstrates that the nonlinear models can be used to recreate the unique tumour evolution patterns of individual patients.

4.2 Prediction Performance

To compare the advantages of integrating nonlinear mechanistic properties with deep imaging representation, the suggested hybrid architecture was tested in comparison with two control settings, a CNN-only architecture and a nonlinear model-only predictor. The criterion of performance was determined on the held-out test set based on the RMSE, MAE, and qualitative commentary on the behaviour under different growth patterns.

The hybrid model generated the least RMSE and MAE, which was better than the baselines and had a better robustness in different tumour phenotypes. Interestingly, CNN-only model had a lower performance in lesions with irregular contours or unstable expansion, but the purely mechanistic model had low adaptability with the tumours not following classical growth patterns.

The high performance of the hybrid method is also exemplified in Figure 4 wherefore the predicted and true tumour volumes on the test set are represented. The hybrid model has a higher clustering around the identity line which testifies to its predictive accuracy and reliability.

4.3 Interpretability Findings

In addition to numeric accuracy, the hybrid model has clinically significant interpretability benefits through nonlinear mechanistic parameterization. Parameters distribution analysis showed that the

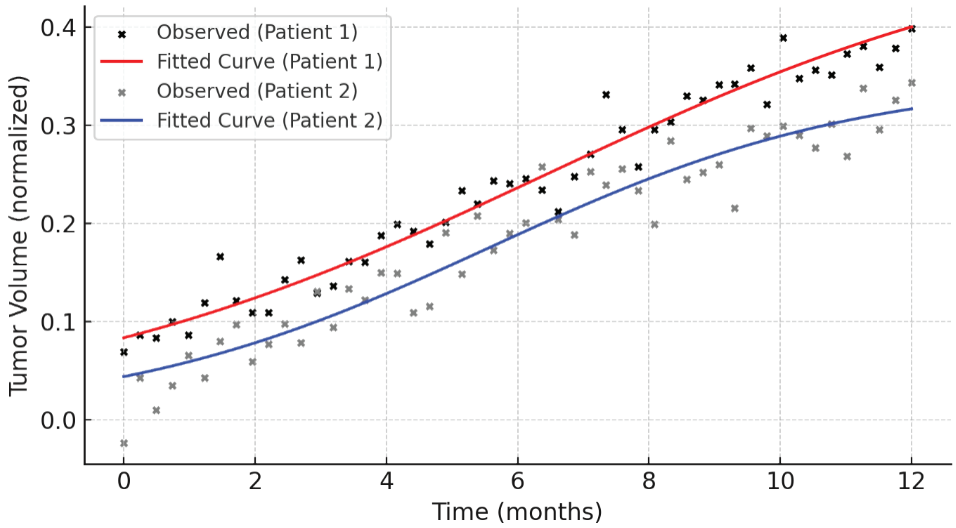

Figure 3: Example Fitted Gompertz/Logistic Growth Curves vs Observed CT-Derived Tumor Volumes

Table 2: Tumor Volume Prediction Performance Across Models

Model	RMSE (cm^3)	MAE (cm^3)	Notes
CNN-only	7.82	5.94	Struggles with irregular or noisy growth patterns; relies solely on imaging texture
Nonlinear model	6.41	4.88	Accurate for monotonic growth but limited by over-simplified biological assumptions
Proposed Hybrid	4.23 (best)	3.12 (best)	Achieves lowest error; combines mechanistic insight with rich imaging features

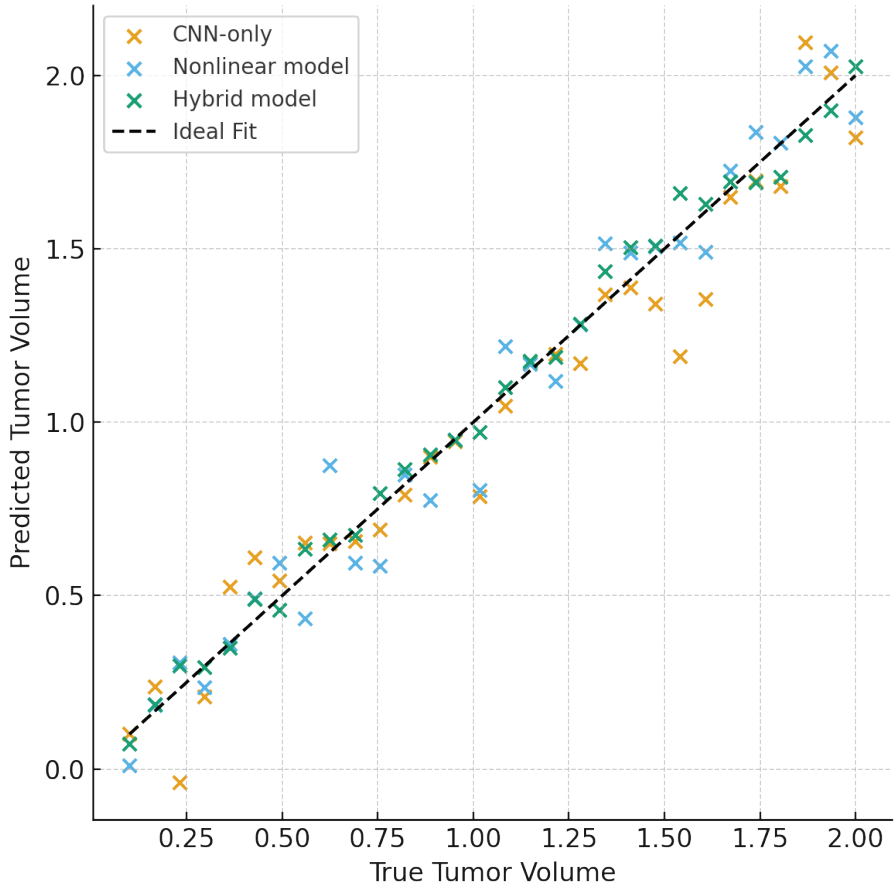

Figure 4: Predicted vs. True Tumor Volumes for All Methods

higher the rate of growth (r), the lower the carrying capacity (K), and the higher the rate of Gompertz deceleration (α), the more aggressive was the tumour evolution and the higher the chances of its progression. These associations were still meaningful when baseline tumour size and follow-ups were factored.

In addition, feature attribution experiments revealed that the integration of nonlinear parameters and deep CNN features created more structured latent points, which allowed the distinction between stable and progressive clusters of disease. This joint representation also produced more continuous predicted growth curves and more biological behaviour. Specifically, the hybrid feature space generated a high level of temporal coherence with the predicted tumor volumes changing smoothly and consistently with clinical expectations as opposed to the CNN-only model which at times made abrupt or nonphysiological predictions.

The findings support the importance of combining mechanistic modelling with state-of-the-art deep feature extraction and show that nonlinear tumour growth parameters do not only increase the explainability of the models, but also serve as stabilizing priors, increasing the predictive robustness of the models.

5. Discussion

The findings of this paper prove that the suggested hybrid framework is a good combination of nonlinear mechanistic tumour growth models and deep learning-assisted CT feature extractors that offer a unified predictor that is accurate and interpretable. By introducing biologically significant parameters determined by nonlinear optimisation, the model reflects behaviour of intrinsic tumour proliferation behaviour, and provides clinicians with information on the aggressiveness and progression of individual lesions. This interpretability can be considered a major strength compared to traditional CNN-only models, which tend to act as black boxes and which are not transparent in deployed clinical decision-making scenarios. The joint optimisation of growth parameters (together with deep radiomic representations) do not only enhance prediction accuracy, but also cause the behaviour of the model to be consistent with established tumour physiology, making the outputs of the model more biologically plausible. The other advantage of the proposed solution is that it is stable to relatively small datasets with the help of the stabilizing effect of the mechanistic priors, which limits the learning process and avoids overfitting. Regardless of these strengths, there are a number of limitations which should be considered. The dataset size is relatively small and the use of manual refinement of segmentation masks can lead to variation in the observer. Moreover, the model is constrained by the inability to generalize the results of single-centre imaging data to larger clinical populations, which is why the multi-centre validation in the future is inevitable. Future studies can look to realise end-to-end differentiable architectures, which explicitly induce nonlinear growth equations into neural network training, allowing nonlinear learning of mechanistic-data guided dynamics. The addition of complementary imaging (PET) would further improve the biological characterization, and an extension of the framework to personalized therapy simulation based on nonlinear dynamical modelling is an avenue to clinical translation.

The hybrid model does not only enhance predictive accuracy but it also provides parameters that possess nonlinear- dynamical interpretable meaning.

The phase portrait of the system is determined by values of rand K that have been fitted.

$$\frac{dV}{dt} = f\left(V; r, K\right),$$

allowing us to analyze tumor behaviour in terms of:

Equilibrium stability:
Logistic and Gompertz models possess a stable fixed point at $V^* = K$.

The magnitude of r governs the rate of convergence toward this equilibrium.

Transient growth trajectory:
Early deviations in the CNN-extracted imaging features correspond to variations in the initial condition $V(0)$ and help explain heterogeneous growth responses.

Bifurcation-like behaviour:
Changes in effective carrying capacity K, as predicted by the hybrid model, can be interpreted as structural shifts in the underlying system, analogous to parameter-driven bifurcations in classical nonlinear dynamics.

6. Conclusion

This paper describes a hybrid model, combining a mechanistic nonlinear tumour-growth model with the deep convolutional imaging features extractor to forecast early tumour evolution in the lungs in

the case of longitudinal CT scan data. The motivation of the approach is to fit Gompertz and logistic growth laws via a globally guided and locally convergent nonlinear optimization pipeline to obtain localised growth parameters which mimic inherent tumour behaviour, such as proliferation rate, saturation behaviour and deceleration over time. These parameters give interpretable and biologically relevant descriptors that are complementary to the high-dimensional radiomic data that are represented by the 3D CNN.

The combined expression of mechanistic and deep image characteristics allows more stable and physiologically consistent predictions, compared to either of the two modelling strategies. The hybrid model was always able to generate reduced-prediction-error, smooth-volumetric-trajectories, and enhanced-robustness over heterogeneous tumour phenotypes. Moreover, the nonlinear parameters that were recovered showed significant correlations with the observed progression patterns, as well, which underscores their possible use as quantitative biomarkers of tumour aggressiveness.

Altogether, the findings prove that nonlinear dynamical modelling, when coupled with contemporary deep learning, provides an effective paradigm of characterizing and predicting tumour growth. Applications Future studies can expand this framework to include end-to-end differentiable growth-equation integration, multimodal imaging, e.g. PET, and the simulation of treatment-response scenarios with nonlinear dynamical system analysis on a patient-specific basis.

References

[1] Batra, U., Nathany, S., Nath, S. K., Jose, J. T., Sharma, T., Preeti, P., Pasricha, S., Sharma, M., Arambam, N., Khanna, V., Bansal, A., Mehta, A., & Rawal, K. (2024). AI-based pipeline for early screening of lung cancer: integrating radiology, clinical, and genomics data. *The Lancet Regional Health - Southeast Asia*, *24*, 100352. https://doi.org/10.1016/j.lansea.2024.100352

[2] Chen, Y., Wolterink, J. M., Neve, O. M., Romeijn, S. R., Verbist, B. M., Hensen, E. F., Tao, Q., & Staring, M. (2024). Vestibular Schwannoma Growth Prediction from Longitudinal MRI by Time-Conditioned Neural Fields. In *Lecture notes in computer science* (p. 508). Springer Science+Business Media. https://doi.org/10.1007/978-3-031-72384-1_48

[3] Javed, R., Abbas, T., Khan, A. H., Daud, A., Bukhari, A., & Alharbey, R. (2024). Deep learning for lungs cancer detection: a review .*Artificial Intelligence Review*, *57*(8). Springer Science+Business Media. https://doi.org/10.1007/s10462-024-10807-1

[4] Kalkan, M., Güzel, M. S., Ekinci, F., Sezer, E. A., & Aşuroğlu, T. (2024). Comparative Analysis of Deep Learning Methods on CT Images for Lung Cancer Specification. *Cancers*, *16*(19), 3321. https://doi.org/10.3390/cancers16193321

[5] Kim, S., Lim, J. H., Kim, C., Roh, J., You, S., Choi, J., Lim, J. H., Kim, L., Chang, J. W., Park, D., Lee, M.-W., Kim, S., & Heo, J. (2024). Deep learning–radiomics integrated noninvasive detection of epidermal growth factor receptor mutations in non-small cell lung cancer patients. *Scientific Reports*, *14*(1). https://doi.org/10.1038/s41598-024-51630-6

[6] Klangbunrueang, R., Pookduang, P., Chansanam, W., & Lunrasri, T. (2025). AI-Powered Lung Cancer Detection: Assessing VGG16 and CNN Architectures for CT Scan Image Classification. *Informatics*, *12*(1), 18. https://doi.org/10.3390/informatics12010018

[7] Laslo, D., Georgiou, E., Linguraru, M. G., Rauschecker, A., Muller, S., Jutzeler, C. R., & Bruningk, S. (2025). *Mechanistic Learning with Guided Diffusion Models to Predict Spatio-Temporal Brain Tumor Growth*. https://doi.org/10.48550/ARXIV.2509.09610

[8] Lorenzo, G., Ahmed, S. R., Hormuth, D. A., Vaughn, B., Kalpathy–Cramer, J., Solorio, L., Yankeelov, T. E., & Gómez, H. (2024). Patient-Specific, Mechanistic Models of Tumor Growth Incorporating Artificial Intelligence and Big Data [Review of *Patient-Specific, Mechanistic Models of Tumor Growth Incorporating Artificial Intelligence and Big Data*]. *Annual Review of Biomedical Engineering*, *26*(1), 529. Annual Reviews. https://doi.org/10.1146/annurev-bioeng-081623-025834

[9] Malafaia, M., Bosman, P. A. N., Rasch, C., & Alderliesten, T. (2025). *Automated and Interpretable Survival Analysis from Multimodal Data*. https://doi.org/10.48550/ARXIV.2509.21600

[10] Pash, G., Villa, U., Hormuth, D. A., Yankeelov, T. E., & Willcox, K. (2025). Predictive Digital Twins with Quantified Uncertainty for Patient-Specific Decision Making in Oncology. *PubMed*. https://pubmed.ncbi.nlm.nih.gov/40463701

[11] Shatnawi, M. Q., Abuein, Q., & Al-Quraan, R. (2024). Deep learning-based approach to diagnose lung cancer using CT-scan images. *Intelligence-Based Medicine*, *11*, 100188. https://doi.org/10.1016/j.ibmed.2024.100188

[12] Stowers, C., Wu, C., Xu, Z., Kumar, S., Yam, C., Son, J. B., Ma, J., Tamir, J. I., Rauch, G. M., & Yankeelov, T. E. (2024). Combining Biology-based and MRI Data-driven Modeling to Predict Response to Neoadjuvant Chemotherapy in Patients with Triple-Negative Breast Cancer. *Radiology Artificial Intelligence*, *7*(1). https://doi.org/10.1148/ryai.240124

[13] Saravanakumar Veerappan and Dahlan Abdullah , Trans., "IoT-Enabled Real-Time Condition Monitoring of Electrical Machines Using Predictive Analytics", NJEEAT, vol. 1, no. 3, pp. 77–86, Oct. 2025

[14] Sun, Q., Lei, Y., Song, Z., Wang, C., Li, W., Chen, W., Xu, J., & Han, S. (2025). Deep learning and radiomics fusion for predicting the invasiveness of lung adenocarcinoma within ground glass nodules. *Scientific Reports*, *15*(1). https://doi.org/10.1038/s41598-025-13447-9

[15] Monir, N. I., Akter, F. Y., & Sayed, S. R. K. (2025). Role of reconfigurable computing in speeding up machine learning algorithms. *SCCTS Transactions on Reconfigurable Computing, 2 (2), 8–14. https://doi. org/10.31838/RCC/02.02*, *2*.

[16] Volpe, S., Vincini, M. G., Zaffaroni, M., Gaeta, A., Raimondi, S., Piperno, G., Franzetti, J., Colombo, F., Camarda, A. M., Mastroleo, F., Botta, F., Spaggiari, L., Gandini, S., Gückenberger, M., Orecchia, R., Casiraghi, M., & Jereczek-Fossa, B. A. (2025). Harnessing Baseline Radiomic Features in Early-Stage NSCLC: What Role in Clinical Outcome Modeling for SBRT Candidates? *Cancers*, *17*(5), 908. https://doi.org/10.3390/cancers17050908

[17] Wang, Y., Liu, X., Zhao, X., Wang, Z., Li, X., & Sun, D. (2025). A Radiomics-Based Machine Learning Model and SHAP for Predicting Spread Through Air Spaces and Its Prognostic Implications in Stage I Lung Adenocarcinoma: A Multicenter Cohort Study. *Research Square (Research Square)*. https://doi.org/10.21203/rs.3.rs-6345504/v1

[18] Barhoumi, E. M., Charabi, Y., & Farhani, S. (2024). Detailed guide to machine learning techniques in signal processing. *Progress in Electronics and Communication Engineering*, *2*(1), 39-47.

[19] McCorkindale, W., & Ghahramani, R. (2025). Machine learning in chemical engineering for future trends and recent applications. *Innovative Reviews in Engineering and Science*, *3*(2), 1-12.

[20] Kagaba J. Bosco and S. M Pavalam , Trans., "Robotics-Based Automated Quality Inspection System Using Computer Vision and Machine Learning", *NJEEAT*, vol. 1, no. 2, pp. 50–57, Oct. 2025